Optimizing Spatially Embedded Networks for Synchronization

Markus Brede[1]

[1]CSIRO Centre for Complex Systems Science, Canberra, ACT 2602, Australia
Markus.Brede@csiro.au

Abstract

In this paper we consider the problem of organizing networks of spatially embedded oscillators to maximize the propensity for synchronization for limited availability of wire, needed to realize the physical connections between the oscillators. We consider two extensions of previous work (Brede, 2010b): (i) oscillators that can flexibly arrange in space during the optimization process and (ii) a generalization to weighted networks. In the first case, we discuss the emergence of spatially and relationally modular network organizations, while in the second case the emphasis of our analysis is on link heterogeneity and the particular organization of strong and weak links that facilitates synchronization in space.

Introduction

Probably starting with Huygens observation of synchronized motions among nearby pendula clocks, synchronization phenomena have long attracted much interest among physicists. Synchronization is ubiquitous in the biological (Winfree, 1980) and in the engineered world (Blekhman, 1988): fireflies that flash in unison, cardiac pacemaker cells, rhythms in the brain or power stations and laser systems are just a few examples (Arenas et al., 2008; Manrubia et al., 2004). All of these systems are distributed coupled systems that can be described by complex networks. Recent findings, that many such networks have highly non-trivial topologies have given rise to a wave of studies about synchronization on complex networks.

One overriding question in this research has been to identify characteristics of network topology that are correlated with enhanced or poor synchronization characteristics. Even though such a statistical characterization has caveats (Atay et al., 2006), important findings have resulted, which allow a rough "rule of thumb" characterization of a networks' propensity for synchronization. Many factors that influence synchronization have been identified: homogeneous network topologies such that every node receives the same strength of an 'in-signal' (Donetti et al., 2005; Motter et al., 2005; Hwang et al., 2005; Chavez et al., 2005; Nishikawa and Motter, 2006b; Brede, 2010c; Nishikawa and Motter, 2010), an 'entangled' structure that does not allow for separate communities of nodes (Donetti et al., 2005), short pathlengths (Watts and Strogatz, 1998) and disassortative degree mixing are just a few examples. Even though optimal network topologies have thus been well-classified, understanding the role of constraints on the network topology and the varying trade-offs between the mentioned characteristics still pose a challenging problem.

One natural source of constraints on network organization is the spatial embedding typical to almost all application systems. The biological fitness (or in an engineering context, a system's optimality) is then not only determined by it's synchronization properties, but also by cost factors associated with requirements to realize the physical connections in space that are needed to establish the coupling. If one considers a system without the spatial embedding, this synchronization cost is related to the number (and possibly weight) of links. In fact, for this case it has been shown that optimal synchronization can be achieved for minimized cost (Nishikawa and Motter, 2006a). However, for spatially embedded networks the cost to establish linkages is a combination of the number and length of links: It can be seen as the length of a wire needed to realize the network links in space.

The problem of optimal synchronization in space has recently been addressed (Brede, 2010b), finding that over a large range of parameters synchrony-optimal networks are small worlds with power law distributed link length. The more severe spatial constraints, the steeper the decay of the power law describing the link length distribution. For several reasons this is an important finding: small worlds with power law distributed link length have been found in neurological networks (Schüz and Braitenberg, 2002), the (physical) internet (Yook et al., 2002) or networks of wire in electronic circuits (Zarkesh-Ha et al., 2000) – all systems where synchronization plays a role. Moreover, random walks on such particular small worlds establish fractal movements patterns in the underlying space, which could have relevance for optimal search (or foraging) patterns (Viswanathan et al., 1999).

Optimization and evolutionary algorithms have a natural place in this research, since they allow for the numerical construction of networks with enhanced synchronization characteristics. Further, apart from the scientific problem setting, many of the biological systems, like the brain, where synchronization plays a role, are systems that have evolved to their current state over a long period of time. Synchronization very likely has played a role in their evolution, such that one can imagine an algorithm that optimizes as networked system for enhanced synchronization as a model to mimick this evolution process.

In this paper we discuss two natural extensions of the abovementioned study Brede (2010b) and investigate whether the power law distributions that classify optimal networks persist in these more general situations as well. First, after a short description of the framework and methodes we employ, we consider optimal synchronization in systems where the nodes are not fixed in space, but are free to change their relative arrangement during the optimization for synchrony-enhancement. Second, in the next following section, we consider the case of synchrony-optimal weighted networks in space. The paper concludes with a section that summarizes our results and puts them into a more general context.

The Model

We investigate identical synchronization in systems of N coupled oscillators, the collective dynamics of which is given by

$$\dot{x_i} = f(x_i) + \sigma \sum_j A_{ij}(g(x_j) - g(x_i)). \quad (1)$$

In the above equation, the function f describes the dynamics of the individual oscillators (without coupling), the matrix A_{ij} is the adjacency matrix of the coupling network, σ the coupling strength and the function g characterizes the so-called 'inner coupling', i.e. defines how the oscillators influence each other. The equation can be rewritten as $\dot{x_i} = f(x_i) + \sigma \sum_j L_{ij} g(x_j)$, which introduces the graph Laplacian matrix belonging to the adjacency matrix A via $L = I - A$, where $I = (\delta_{ij})$ is the identity matrix. It is important to note that in all scenarios considered in this paper A is symmetrical and has only positive entries, such that all eigenvalues of L are real and nonnegative. Without loss of generality we will further restrict the study to connected networks. In this case L has exactly one zero eigenvalue and one can label the eigenvalues of L in ascending order $0 = \lambda_1 < \lambda_2 < ... < \lambda_N$.

A big step forward in understanding identical synchronization in the system (1) is due to Pecora and Carroll (Pecora and Carroll, 1998), who analyzed the stability of the synchronized state $\dot{x} = f(x)$. In (Pecora and Carroll, 1998) they were able to show that for a large class of oscillators f and inner couplings g, the stability of the fully synchronized state is determined by the eigenratio $e = \lambda_N / \lambda_2$. Importantly, the eigenratio analysis abstracts from the details of the underlying dynamics (i.e. the function f) and allows an analysis of the influence of the connection architecture (given by the adjacency matrix A of the coupling network) for a general class of dynamics. Essentially, a network has a superior propensity to synchronize when the spread of the eigenvalues is as small as possible – or e close (or identical) to one.

The spatial component of the model is introduced by allocating nodes spatial locations $l_i > 0$ in a one-dimensional space with periodic boundary conditions. Then, if $l_{\max} = \max_i(l_i)$, a spatial distance metric can be defined via $d(i,j) = \min(|l_i - l_j|, l_{\max} - |l_i - l_j|)$ and the amount of 'wire' needed to connect the nodes in space according to a network A is

$$W = \sum_{i<j} A_{ij} d(i,j). \quad (2)$$

As already suggested in (Brede, 2010b), spatial constraints on the network evolution can be considered via the optimization of the synchronization properties of the network for limited amount of wire W. Alternatively, a more elegant framework can be the minimization of an energy-like goal function that combines considerations of synchronization properties with the minimization of the amount of wire used via

$$E = \beta W + (1 - \beta) e, \quad (3)$$

where the trade-off parameter $0 \leq \beta \leq 1$ weighs the importance of wire minimization versus that of enhanced synchronization during network evolution. Compare also (Mathias and Gopal, 2001; Sole and Ferrer i Cancho, 2003; Brede, 2008) for other studies where a similar framework has been used in different contexts.

Importantly, if $\beta = 1$ the goal function is solely determined by the amount of wire. The minimum of E then corresponds to a network configuration in which only spatial nearest neighbours are connected – a configuration which is known to have very poor synchronization properties. On the other hand, when $\beta = 0$ considerations of wire and the underlying space play no role in the minimization of E. This case corresponds to (Donetti et al., 2005) (and apart from (Brede, 2010b) all other studies of optimal identical synchronization on networks, cf. (Arenas et al., 2008)). Note, that if one decreases β towards $\beta = 1$, the 'severity' of spatial constraints in the network evolution process can be tunedx.

We approach the problem of minimizing (3) via a numerical optimization scheme using simulated annealing. The scheme consists of a series of rewiring suggestions, which

are accepted if they improve the fitness or energy (3) of the network configuration. Prototypically, even though step 2 is modified according to the slightly more general problem definitions in section III and IV, we employ the following scheme:

1. Start with an Erdös-Rényi random graph with exactly L links and distribute oscillators uniformly in space at locations $l_i = i$, $i = 0, ..., N-1$. Calculate the fitness of the first network configuration.

2. Rewire one or several links. Calculate the resulting network fitness E' of the modified configuration according to Eq. (3) and accept if $E' < E$ or with probability $p \propto \exp(-\nu(E - E'))$ otherwise. The inverse temperature ν of the annealing procedure is gradually reduced as the optimization progresses.

3. Terminate the algorithm if no large improvement in E was achieved during a certain number of iterations.

Because for larger networks the optimization procedure did not result in a unique optimal configuration (and due to the inherent difficulty of making sure a numerical optimization approach actually achieved a global optimum) we typically constructed around $R = 100$ optimal network configurations by the algorithm. In both situations considered in more detail in the following sections, all the near-optimal networks proved to be structurally very similar, which underlines that the findings we will discuss below are robust. The structural similarity of the constructed networks also gives support to the approach to optimize linear combinations of the quantities of interest rather than to construct the full Pareto front in a multi-objective optimization approach.

Optimal synchronization with flexible node locations

In the previous study (Brede, 2010b), optimal synchronization was considered for the case of spatial networks with nodes that have fixed locations in space. Here, we extend the framework and consider nodes that can arrange freely in space during the optimization procedure. However, without further constraint this would clearly imply that all nodes drift to one location, thus allowing for complete connectivity without cost of wire. To prevent this and to study which arrangement of nodes is optimal, we introduce a further constraint, requiring that the average spatial distance of the nodes remains the same during the optimization, i.e. that

$$D = \frac{2}{N(N-1)} \sum_{i<j} d(i,j) = \text{const.} \tag{4}$$

Accordingly, we then modify step 2. of the optimization procedure of the previous section, in which we now also include suggestions for location changes of nodes $l_i \rightarrow$

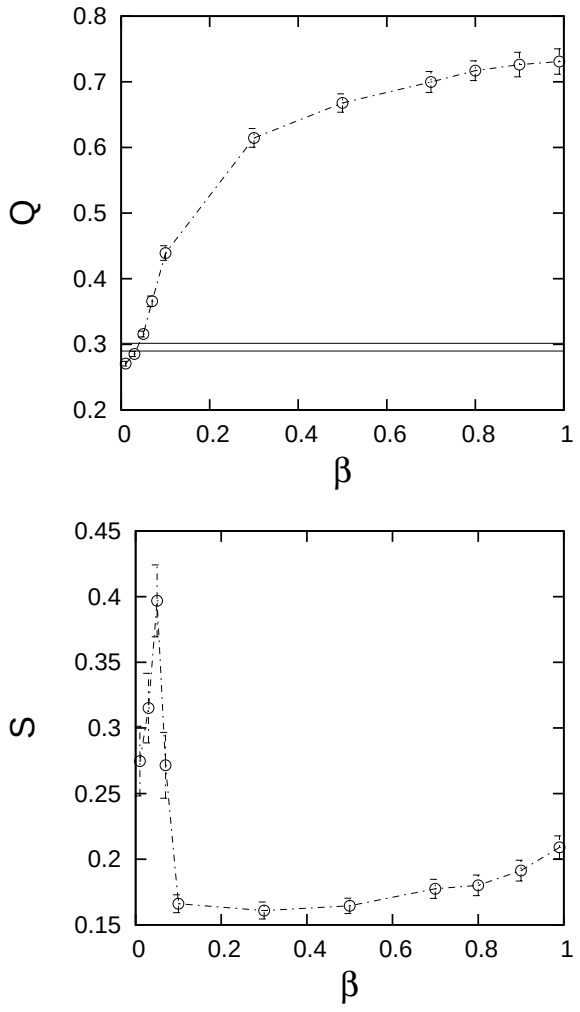

Figure 2: Dependence of the relational (top) and spatial modularity (bottom) of the evolved networks and spatial arrangements on the trade-off parameter β: For reference, the horizontal lines indicate the range the respective quantities would assume for a an Erdös-Rényi random graph whose nodes are uniformly distributed in space. In the plot of the spatial modularity the lines are omitted for scaling reasons, one has $S < 10^{-3}$ in that case. All data are for networks of $N = 100$ nodes with $L = 400$ links and are averaged over 100 different initial configurations for each β.

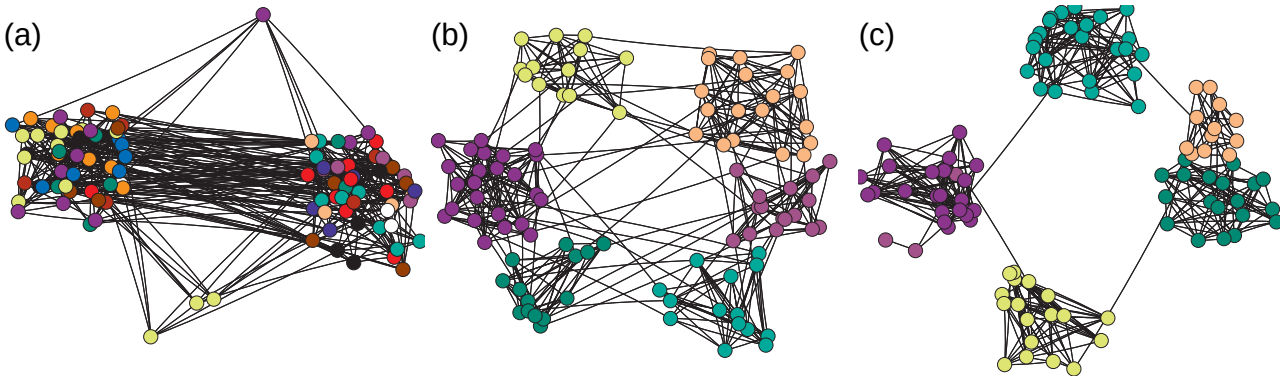

Figure 1: Examples of evolved networks for different trade-offs between cost of wire and desireability for superior synchronization: (a) $\beta = 0.01$ (very low cost of wire), (b) $\beta = 0.5$ (balanced costs for wire and synchronization), and (c) $\beta = .01$ (very high cost of wire). The networks are of size $N = 100$ and contain $L = 400$ links. In the figure vertices have been colored according to the modules they belong to (modularities are $Q = .26$ for (a) and $Q = 0.71$ and $Q = 0.78$ for (b) and (c)). The spatial locations roughly correspond to the evolved spatial locations of the nodes during the optimization, however a random number was added to make vertices distinguishable.

$l_i + \Delta l_i$. After such a location change suggestion, D' of the modified configuration is calculated and all locations l_i, $i = 1, ..., N$ are scaled by D/D', i.e. we set $l_i \rightarrow D/D' l_i$, to ensure $D = const.$ during the optimization.

Figure 1 gives some illustrations of example networks constructed by optimizing the energy (3) for three different scenarios: (a) very low cost of wire, (b) balanced cost of wire and desirability of superior synchronization and (c) expensive wire. The figures already illustrate a number of differences in network organization to the results reported in (Brede, 2010b). First, it becomes apparent that two distinct classes of link lengths can be identified: short links and long links. The gap between these two types of links depends on the trade-off parameter β – it is large when wire is very costly or very inexpensive and relatively small when the cost of wire and synchronization needs are balanced. Second, depending on β, the network organization can become distinctly modular. Third, it becomes apparent that the spatial locations of nodes become distinctly clustered, such that the nodes either crowd at two (for the case of low β) or more (for intermediate and large β) spatial locations.

Modularity is an important property of many real-world networks, see, e.g. (Girvan and Newman, 2004). It denotes the fact that networks are organized into communities of nodes that are more strongly connected to each other than to the rest of the network. A widely accepted measure to quantify network modularity has been introduced in (Girvan and Newman, 2004)

$$Q = \sum_m [L_m/L - (d_m/2L)^2]. \quad (5)$$

In eq. (5) the index m runs over all network communities, L_m denotes the number of links within a module, d_m the sum of all degrees of nodes in module m and $L = \sum_{i<j} A_{ij}$ the overall number of links in the network. Several algorithms to identify modules in networks have been suggested. Because the networks that we evolved above are relatively small, we use extremal stochastic optimization (Duch and Arenas, 2005) to calculate Q and identify modules. As an example of results of the module identification see figure 1a-c, where we have identified modules by the colors of the nodes. The respective values of the modularity measure Q are given in the caption of the figure.

For an analysis of the spatial modularity of the evolved networks we have analyzed the correlation function $G(x)$ that gives the density of nodes at distance x from an average node. A plot of G for different trade-off parameters allows the distinction between two scenarios (see also figure 1): (i) $G(x)$ is u-shaped with two peaks at $x = 0$ and $x = l_{\max}/2$ and a flat trough in between which clearly corresponds to an arrangement of nodes into two clusters separated by the maximum distance and (ii) $G(x)$ has one sharp peak at $x = 0$ which corresponds to an arrangement into several spatial clusters. A more thorough investigation of the link length distributions and widths of the peaks of the correlation function G suggests a cut-off of around $\Delta x = 0.01$, links with length $l \leq \Delta x$ being classified as 'short' and links with lengths $l > \Delta x$ being 'long'. Then, one can define a spatial cluster as the maximum number of nodes with distances less than Δx or

$$S = \int_0^{\Delta x} G(x) dx. \quad (6)$$

Thus, our spatial modularity measure is the average fraction of nodes in one spatial '0.01-cluster'.

In the top and bottom panel of figure 2 we present a more detailed analysis of the modularities of the evolved

networks. A short glance at the spatial modularity reveals two typical structural regimes that are separated by a sharp transition at around $\beta_c = 0.1$. Below the transition for $\beta < \beta_c$ the evolved networks show a clear two spatial cluster regime, both clusters being separated by the maximum spatial distance. A comparison of the respective network modularity to that of random networks (indicated by the two lines in Fig. 2) shows that the network modularity is suppressed in this regime. The spatial clustering is thus not correlated with a corresponding network modularity. As an aside, it is also clear that $S \to \Delta x l_{\max}/(2N)$ (uniform distribution of nodes in space) as $\beta \to 0$. From this argument one understands that the spatial modularity peaks and then declines again in the $\beta < \beta_c$-regime.

Above the transition, with $S > 0.15$ the networks are still strongly spatially clustered, albeit the spatial clustering is strongly reduced in comparison to the $\beta > \beta_c$ case. This indicates the presence of multiple ($\approx 1/S$) smaller spatial clusters. In contrast to the case of $\beta < \beta_c$, the spatial clustering goes hand in hand with strong network modularity. Closer investigation reveals that membership of nodes to spatial modules is correlated with membership in network modules, which already hints to a mechanism of module formation. Clearly, in terms of wire it is 'cheap' to connect near-by nodes. Thus, there is a positive feedback mechanism: near-by nodes are likely to move closer to each other. This makes it cheaper to connect them and fosters the establishment of connections to other near-by nodes, thus facilitating network modularity. Network modularity in turn causes more spatial clustering since moving nodes of the same module spatially closer to each other further reduces the cost of wire.

Hence, allowing for flexible node locations during the network evolution leads to the formation of very different optimal network organizations than described in (Brede, 2010b), namely a very clear two mode structure of the link length distribution compared to the presence of all length scales leading to the power laws observed in (Brede, 2010b). Interestingly, the additional degree of freedom leads to the emergence of spatial clustering and modular network organization, and, associated with it, separate time-scales of synchronization processes (Arenas et al., 2006). For a more detailed discussion of these networks the reader is referred to (Brede, 2010d).

Optimal synchronization in weighted networks

In this section we are interested in weighted synchrony-optimal networks in space. In order to understand the influence of weights and spatial arrangement separately, like (Brede, 2010b) we consider nodes at fixed spatial locations $l_i = i$, $i = 0, ..., N-1$ that do not change position during the optimization. However, links A_{ij} are now not restricted to binary values, but can assume any weight $A_{ij} \geq A_{\min}$. The lower cut-off $A_{\min}$ was introduced for reasons of limited computation time and limited numerical precision in the eigenvalue calculations.

A larger coupling A_{ij} between two nodes allows for better synchronization between the nodes i and j. However, larger coupling also requires more wire and thus implies a larger cost for the physical connection of the nodes in space. A reasonable assumption is that the connection strength between two nodes is proportional to the thickness of the wire to connect the nodes. Hence, assuming a wire of constant density, the cost C of the wire is proportional to its length in space and the connection strength, such that $C_{ij} = d(i,j)A_{ij}$. One may also think of more general formulations for the cost function like $C_{ij} = d_{ij}h(A_{ij})$, which we leave for future work.

If one considers optimal weighted networks in the framework of the stability analysis of the synchronized state which leads to the eigenratio $e = \lambda_N/\lambda_2$ as a measure for synchronization, it is important to note that for any coupling network with Laplacian matrix L one has $e(kL) = e(L)$ for any scaling factor $k > 0$. Also, one has $e = 1$ for the fully connected graph with $L^F_{ij} = 1$ for $i \neq j$ and $L^F_{ii} = -N + 1$. Thus, for any coupling network configuration in space with $E(\beta) > 1 - \beta$ one can always choose a small enough factor k, such that the fully connected graph with link weights k has a smaller energy. As one easily realizes, however, this is a consequence of the different scaling of both contributing factors to Eq. (3). A more adequate problem definition that avoids this scaling issue is to introduce a scaled cost of wire via

$$C_{ij} = \frac{L \sum_{i<j} d(i,j)A_{ij}}{\sum_{i<j} A_{ij}}, \tag{7}$$

where $L = \sum_{i<j} H(A_{ij})$ and $H(x) = 1$ if $x > A_{\min}$ and $H(x) = 0$ otherwise. In Eq. (7) every link contributes to the cost with its weight relative to the average weight of links $\overline{w} = \sum_{i<j} A_{ij}/L$. One can then substitute (7) into Eq. (3) and obtains

$$E(\beta) = \beta \sum_{ij} C_{ij} + (1-\beta)e. \tag{8}$$

In fact, since $\overline{w} = 1$ for binary networks the definition (8) coincides with (3) for this case.

To construct optimal weighted networks in space we modify step 2. of the network evolution algorithm outlined before, by now considering weight transfers between links in the network, i.e. for randomly selected i, j with $A_{ij} \geq \epsilon$ and randomly selected k, l we suggest a reconfiguration $A_{ij} \to A_{ij} - \epsilon$ and $A_{kl} \to A_{kl} + \epsilon$. The suggested amount of the weight transfers ϵ is randomly selected from the interval $[A_{\min}, s]$. Best performance of the algorithm could be achieved when one starts with $s \approx 2\overline{w}$ and then decreases s linearly during the optimization.

Figure 3 displays some illustrations of typical optimal weighted networks for various trade-off parameters β. As

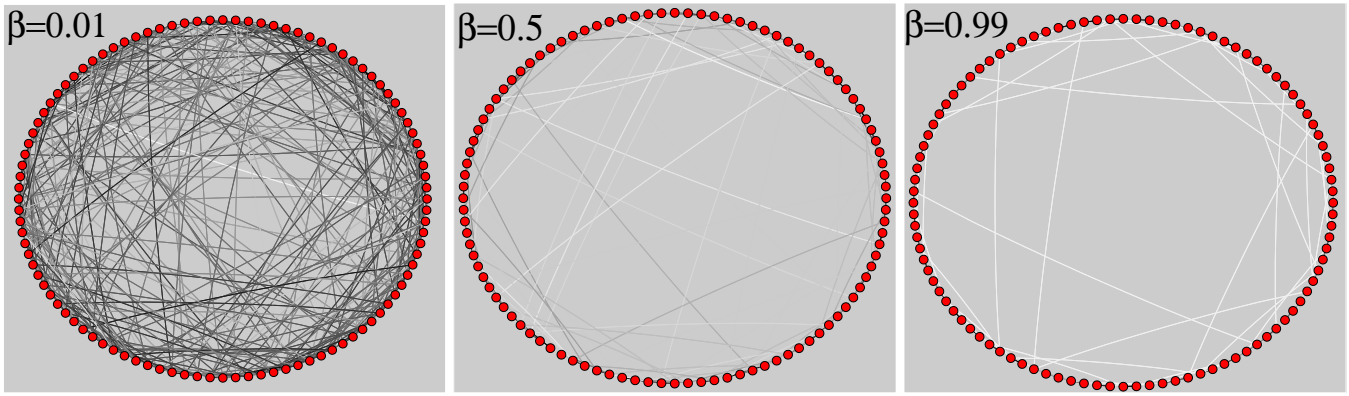

Figure 3: Illustration of some example weighted optimized networks for trade-off parameters $\beta = 0.01, 0.50$ and 0.99. The shade of grey of the links corresponds to link weight, weak links are white and strong links black. The background is shaded in grey to demonstrate the presence of very weak long links.

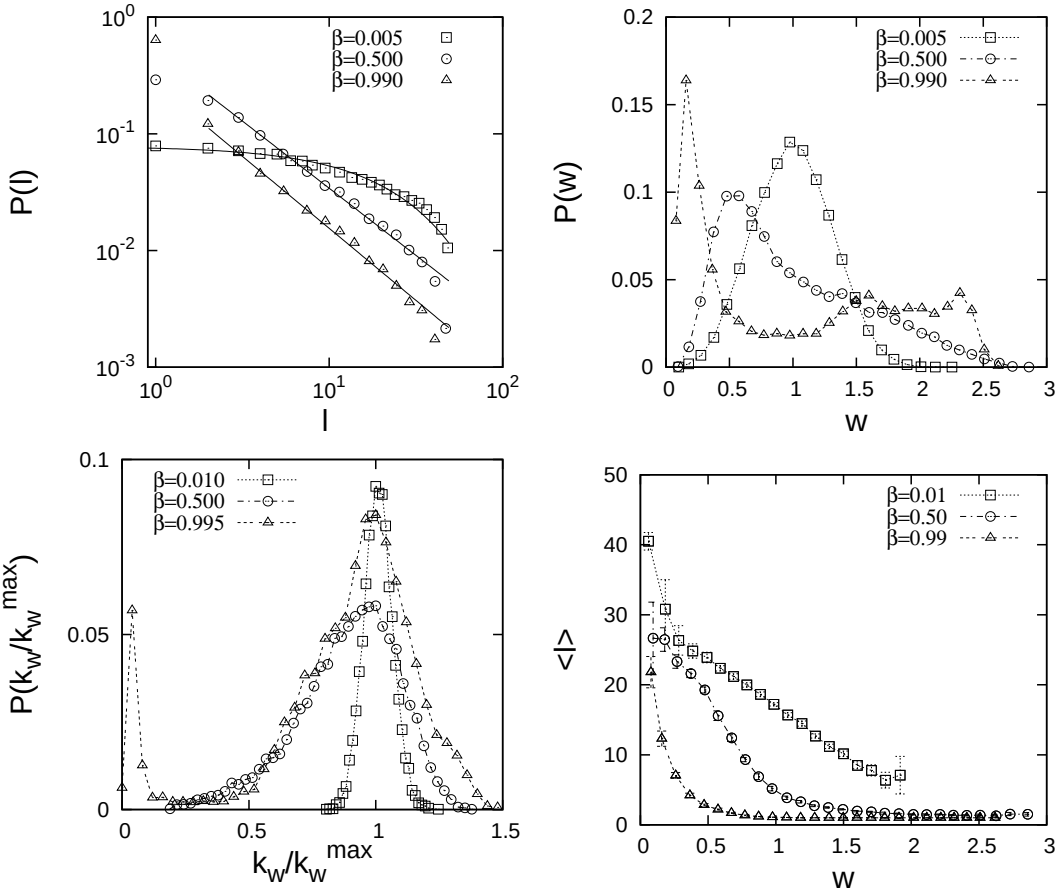

Figure 4: Network statistics for typical optimal weighted networks for small ($\beta = 0.005$), intermediate ($\beta = 0.5$) and large ($\beta = 0.99$) trade-off parameter: (top left) distribution of link lengths, (top right) distribution of link weights, (bottom left) distribution of weighted degrees (normalized by the respective maxima of the distributions for different β) and (bottom right) dependence of link length on link weight. The data have been averaged over 100 optimized networks of size $N = 100$.

one would expect, links are relatively dense and strong for low β and become increasingly scarcer and weaker when β is increased. Importantly, however, a careful inspection of the figures reveals that in all situations strong and weak links are present: strong links typically connecting spatially close nodes whereas weak links establish long-range connections.

For a more detailed investigation we constructed ensembles of 100 optimized networks of $N = 100$ nodes for various trade-off parameters β. To understand the pecularities of a given network, comparisons to suitable randomized null models are necessary. For the case of spatially embedded networks of interest here, a possible null model are (connected) networks with the same spatial constraint, i.e. random weighted networks that use the same amount of wire than the original network. Such networks can easily be constructed by randomly shifting small amounts of wire density between links (and to link vacancies), which are accepted as long as they (i) leave the network connected and (ii) leave the amount of wire used constant within a certain tolerance interval.

As a reference point for comparison below it is of interest to understand the architecture of such randomized networks. As connections between nodes are random, they have binomial degree distributions. The distribution of link weights is centred around a mean with steeply decaying tails towards much larger or much smaller weights. Further, link length distributions are exponential and, by construction, link weight is independent of link length.

In Figure 4 some network statistics for typical situations for low, intermediate and large β are displayed. The top left panel gives the distribution of link lengths in the optimized networks. Even though the system size is relatively small, it is apparent that the optimal link arrangements for strong and intermediate spatial constraint are characterized by power law tails $P(l) \propto l^{-\alpha}$ in the link length distribution. Best fits yield $\alpha = 1.23 \pm 0.02$ for $\beta = 0.99$ and $\alpha = 1.15 \pm 0.02$ for $\beta = 0.5$ and the organization is thus clearly distinct from the random null model.

The decay of the tails with growing link size becomes steeper, the more emphasis is put on link economy. In contrast, when spatial contraints play only a minor role for $\beta = 0.005$, the link length distribution is fitted well by an exponential function. This function, however, declines more strongly for large link length than expected from the null model.

Networks in the power law regime are very sparse and not very far from being tree-like, such that the power laws in the link length distributions appear consistent with a hierarchical organization in space (Brede, 2010a). The exponents of the power laws, however, are distinctly smaller than $\alpha = 2$ which has been found to be the optimal arrangement for discrete networks that optimize a trade-off between cost of wire and network distance.

Of interest is also the distribution of weights, cf. figure 4 (top right). Whereas this distribution is only slightly skewed for small β, increasing the cost of wire leads to increasingly more asymmetrical skewed distributions. Finally, for very large β, the distributions become bimodal – strongly spatially constrained synchrony-optimal networks are thus comprised of clearly distinct strong and weak links. How is the arrangement of these links? The answer is already suggested by the network illustrations in figure 3. A more thorough statistical analysis is provided in figure 4 (bottom right), in which we plot the dependence of the average length of a link on its weight. For all situations investigated, low, intermediate and strong spatial constraints, a clear picture emerges. Strong links typically connect spatially close nodes whereas weak links establish long-range connections.

The increasing skewness of the link weight distributions with increasing spatial constraints is also reflected in the distributions of (weighted) degrees $k_{\mathrm{W}}(i) = \sum_j A_{ij}$, cf. figure 4 (bottom left). When spatial constraints only play a small role, the distribution of weighted degrees is very narrow and almost bell-shaped, as one would expect from previous studies of unconstrained networks which have highlighted the important role of in-signal homogeneity for superior synchronization (Motter et al., 2005). With increasing influence of spatial constraints, however, the distribution becomes more and more skewed towards lower degrees and finally becomes bimodal at around $\beta = 0.95$.

Summary and conclusions

In this paper we have explored three scenarios for synchrony-optimal undirected networks subject to a tuneable degree of spatial constraints, which are parametrised by a cost-of-wire parameter β. We started with the model of (Brede, 2010b) of unweighted networks connecting nodes with fixed spatial locations. In this case, over a wide range of constraints β, such networks are characterized by link size arrangements that obey a power law $P(l) \propto l^{-\alpha}$ with an exponent α that becomes larger the stronger the influence of spatial constraints on network formation.

Next, in the same model, we explored optimal network configurations that arise when nodes are free to change their relative arrangement in space during the optimization. Two regimes of optimal networks separated by a sharp transition at some critical trade-off parameter β_c can be distinguished. For low $\beta < \beta_c$, nodes are found to cluster into two spatial groups separated by the maximum spatial distance. Above the critical β, nodes arrange themselves into multiple spatial clusters that conincide with network modules. These findings are of interest, since they point out that network arrangements normally not associated with superior synchronization can become optimal, when spatial constraints are important.

In the third part of the paper we have gone back to the scenario of (Brede, 2010b), but now considered weighted undirected networks. The results essentially corroborate

that spatially constrained synchrony-optimal networks are characterized by power-law link length distributions. However, as the networks are weighted, when spatial constraints are important, a clear separation of strong and weak links emerges as well. We typically find that strong links connect spatially close nodes, whereas weak links establish remote connections.

Acknowledgements

This research was undertaken on the NCI National Facility in Canberra, Australia, which is supported by the Australian Commonwealth Government.

References

Arenas, A., Díaz-Guilera, A., Kurths, J., Moreno, Y., and Zhou, C. (2008). Synchronization in complex networks. *Physics Reports*, 469:93.

Arenas, A., Diaz-Guilera, A., and Perez-Vicente, C. J. (2006). Synchronization reveals topological scales in complex networks. *Physical Review Letters*, 96:114102.

Atay, F. M., Biyikoglu, T., and Jost, J. (2006). Network synchronization: Spectral versus statistical properties. *Physica D*, 224:35–41.

Blekhman, I. (1988). *Synchronization in Science and Technology*. ASME Press, New York.

Brede, M. (2008). Locals vs. global synchronization in networks of non-identical kuramoto oscillators. *European Physics Journal B*, 62:87.

Brede, M. (2010a). Coordinated and uncoordinated optimization of networks. *Physical Review E*, 81:066104.

Brede, M. (2010b). Optimal synchronization in space. *Physical Review E*, 81:025202(R).

Brede, M. (2010c). Optimal synchronization in strongly connected directed networks. *European Physics Journal B*, 74:217.

Brede, M. (2010d). Small worlds in space: Synchronization, spatial and relational modularity. *Europhysics Letters (in press), available online: arXiv:1006.2894v1*.

Chavez, M., Hwang, D.-U., Amann, A., Hentschel, H. G. E., and Boccaletti, S. (2005). Synchronization is enhanced in weighted complex networks. *Physical Review Letters*, 94:218701.

Donetti, L., Hurtado, P. I., and Muñoz, M. A. (2005). Entangled networks, synchronization, and optimal network topology. *Physical Review Letters*, 95:188701.

Duch, J. and Arenas, A. (2005). Community detection in complex networks using extremal optimization. *Physical Review E*, 72:027104.

Girvan, M. and Newman, M. E. J. (2004). Finding and evaluating community structure in networks. *Physical Review E*, 69:026113.

Hwang, D.-U., Chavez, M., Amann, A., and Boccaletti, S. (2005). Synchronization in complex networks with age ordering. *Physical Review Letters*, 94:138701.

Manrubia, S. C., Mikhailov, A. S., and Zanette, D. H. (2004). *Emergence of Dynamical Order. Synchronization Phenomena in Complex Systems*. World Scientific, Singapore.

Mathias, N. and Gopal, V. (2001). Small worlds: How and why. *Physical Review E*, 63:021117.

Motter, A. E., Zhou, C. S., and Kurths, J. (2005). Enhancing complex-network synchronization. *Europhysics Letters*, 69:334–340.

Nishikawa, T. and Motter, A. E. (2006a). Maximum performance at minimum cost in network synchronization. *Physica D*, 224:77–89.

Nishikawa, T. and Motter, A. E. (2006b). Synchronization is optimal in non-diagonalizable networks. *Physical Review E*, 73:065106.

Nishikawa, T. and Motter, A. E. (2010). Resolving the network synchronization landscape: compensatory structures, quantization, and the positive effect of negative interactions. pages e–print arxiv:0909:2874v1.

Pecora, L. M. and Carroll, T. L. (1998). Master stability functions for synchronized coupled systems. *Physical Review Letters*, 80:2109.

Schüz, A. and Braitenberg, V. (2002). The human cortical white matter: Quantitative aspects of cortico-cortical long-range connectivity. In Schüz, A. and Miller, R., editors, *Cortical Areas: Unity and Diversity*, pages 377–385. Taylor & Francis, London.

Sole, R. V. and Ferrer i Cancho, R. (2003). Optimization in complex networks. In *Statistical Mechanics of Complex Networks,Lecture notes in Physics*, pages 114–125. Springer, Berlin.

Viswanathan, G., Buldyrev, S. V., Havlin, S., da Luz, M. G., Raposo, E., and Stanley, H. E. (1999). Optimizing the success of random searches. *Nature*, 401:911–914.

Watts, D. J. and Strogatz, S. H. (1998). Collective dynamics of 'small-world' networks. *Nature*, 393:440–442.

Winfree, A. T. (1980). *The Geometry of Biological Time*. Springer-Verlag, New York.

Yook, S.-H., Jeong, H., and Barabási, A.-L. (2002). Modelling the internet's large-scale topology. *Proc. Natl. Acad. Sci. U.S.A.*, 99:13382.

Zarkesh-Ha, P., Davis, J. A., and D., M. J. (2000). Prediction of net-length distribution for global interconnects in a heterogeneous system-on-a-chip. *IEEE Trans. Very Large Scale Integr. (VLSI) Syst.*, 8:649.